Phase Diagrams and Aggregation Behavior of Poly(oxyethylene)–Poly(oxypropylene)–Poly(oxyethylene) Triblock Copolymers in Aqueous Solutions

G. Wanka, H. Hoffmann,* and W. Ulbricht

Physical Chemistry 1, University of Bayreuth, D-95440 Bayreuth, Germany

Received December 10, 1993; Revised Manuscript Received March 29, 1994•

ABSTRACT: The aggregation and phase behavior in water of several triblock copolymers of poly(oxyethylene)–poly(oxypropylene)–poly(oxyethylene) [$(EO)_x(PO)_y(EO)_x$] has been studied. The y-values of the compounds ranged from 16 to 70 and the x:y ratios from 0.1 to 2.5. All studied compounds form micelles and lyotropic liquid crystalline phases. For a constant temperature the critical micelle concentrations (cmc) of the compounds decrease exponentially with y. The energy increment for the transfer of a PO group from the aqueous to the micellar state is about (0.25 ± 0.05) kT. The cmc values for all compounds decrease strongly with increasing temperature. As a consequence the solutions undergo a monomer–micelle transition for constant concentration and increasing temperature. This micellization process is associated with a large endothermic heat which is linearly dependent on the size of the PO block. It is concluded that this heat is due to the dehydration of the PO groups, and it is called the heat of micellization ΔH_m. For most of the studied compounds ΔH_m = 3.0 ± 0.5 kJ/mol for one PO group. The large change of the cmc values with temperature can quantitatively be explained by the large ΔH_m values. The sequence of the lyotropic mesophases is mainly determined by the x:y ratio. Systems with x:$y > \approx 0.5$ form spherical micelles for $c >$ cmc. The size of the micelles is independent of the concentration and temperature, if the temperature is about 20 °C above the micellization temperature T_m; in a transition region around T_m the micellar size increases strongly with temperature. Below T_m or the cmc only monomeric block copolymer molecules are present in the solution. At higher concentrations and temperatures solutions with spherical micelles form in a first-order transition a transparent, optically isotropic, highly viscous, and elastic cubic phase. The formation of this cubic phase can be understood by hard-sphere interaction between the aggregates. With further increasing concentrations transitions to hexagonal and to lamellar phases are observed. Samples with a smaller hydrophilic EO block, i.e., with x:$y \approx 0.25$, usually form a hexagonal phase as the first liquid crystalline mesophase, while for systems with ratios x:$y \approx 0.15$ a lamellar phase is found as the first mesophase; samples with x:$y \ll 0.1$ are no longer soluble in water. The lyotropic mesophases show also a thermotropic behavior; i.e., reversible transitions cubic → hexagonal → lamellar or from isotropic solutions to mesophases occur at constant block copolymer concentration with increasing temperatures. The mesophases usually melt at temperatures below 100 °C to systems consisting of one or more isotropic liquid phase.

1. Introduction

It is now well established that block copolymers of the type $(EO)_x(PO)_y(EO)_x$ behave in many ways like normal hydrocarbon surfactants. The compounds are surface active and form micelles and lyotropic liquid crystalline phases. In comparison to normal surfactants these compounds have the peculiarity that their critical micelle concentration (cmc) and their surface activity depend more strongly on temperature than those for the classic nonionic surfactants $C_y(EO)_x$. The cmc' s of the block copolymers can shift several orders of magnitude within a small temperature range. For the commercially used systems the main shift occurs in the temperature region between 20 and 50 °C. The consequence of this is that in moderately concentrated solutions with 1 wt % polymer the block copolymers are present in the monomer state below room temperature and are transformed into micelles at higher temperatures. Usually there is a broad temperature region of about 20 °C in which the transformation occurs. The formation of the micelles is accompanied with a large endothermic heat which can easily be determined by DSC experiments. The heat of micellization is assumed to be due to the dehydration of the propylene oxide groups even though this has not been proven unambiguously. Micellar solutions of block copolymers have been investigated with many different techniques including NMR, static and dynamic light scattering, rheology, fluorescence, and SANS.[1] As a consequence of these many investigations a lot is known about the properties of the micelles. It is usually concluded from these measurements that the core of the micelles consists of PO groups and the aggregation number of globular micelles is determined by the length of the PO block. The core of the micelles is assumed to be free of water, while the EO groups are still hydrated. As a consequence the effective volume fraction of the micelles is generally about a factor of 2–3 larger than the real volume fraction. With increasing temperature above the micellization temperature desolvation of the EO groups continues and the effective volume fraction of the micelles decreases. This is reflected in the phase diagrams.

The picture of a triblock copolymer micelle with dehydrated PO blocks in the core and hydrated EO blocks at the micellar surface is a good model with which most of the experimental data can be explained. Linse and co-workers[1,33,35] developed on the basis of numerical calculations a more refined model which allows also to a certain extent a water penetration into the micellar core and a miscibility of the PO and EO groups; this will be discussed further in the last chapter.

For higher block copolymer concentrations the systems form lyotropic liquid crystalline phases. Since the effective volume of the systems is much larger than the real volume, liquid crystal formation can occur in concentration regions where it is normally not expected for hydrocarbon surfactants. It was shown for the first time by SANS measurements that the gelation process which is observed in some moderately concentrated block copolymer solutions with increasing temperature is actually due to the

• Abstract published in *Advance ACS Abstracts*, June 1, 1994.

0024-9297/94/2227-4145$04.50/0

Table 1. Trade Names, General Formulas, and Average Molar Weights of the Investigated $(EO)_x(PO)_y(EO)_x$ Block Copolymers

block copolymer	general formula	molar weight
L 35	$(EO)_{11}(PO)_{16}(EO)_{11}$	1856
F 38	$(EO)_{42}(PO)_{16}(EO)_{42}$	4640
PF 10	$(EO)_2(PO)_{27}(EO)_2$	1742
PF 20	$(EO)_5(PO)_{27}(EO)_5$	2006
PF 40	$(EO)_{12}(PO)_{27}(EO)_{12}$	2622
PF 80	$(EO)_{73}(PO)_{27}(EO)_{73}$	7990
PE 6100	$(EO)_2(PO)_{30}(EO)_2$	1916
PE 6200	$(EO)_{10.5}(PO)_{30}(EO)_{10.5}$	2660
PE 6400	$(EO)_{13}(PO)_{30}(EO)_{13}$	2900
P 65	$(EO)_{20}(PO)_{30}(EO)_{20}$	3500
PE 6800	$(EO)_{74}(PO)_{30}(EO)_{74}$	8270
F 68	$(EO)_{80}(PO)_{30}(EO)_{80}$	8780
F 88	$(EO)_{100}(PO)_{39}(EO)_{100}$	11062
Vop 32	$(EO)_{63}(PO)_{44}(EO)_{63}$	8096
P 104	$(EO)_{18}(PO)_{58}(EO)_{18}$	4948
L 121	$(EO)_5(PO)_{70}(EO)_5$	4500
L 122	$(EO)_{11}(PO)_{70}(EO)_{11}$	5028
P 123	$(EO)_{20}(PO)_{70}(EO)_{20}$	5820
F 127	$(EO)_{106}(PO)_{70}(EO)_{106}$	13388

formation of a cubic phase.[2] Since then Mortensen et al.[3] have obtained detailed information by SANS on the cubic phase. They showed in particular that these phases can be aligned by shear. Besides the cubic phases, other liquid crystalline phases like hexagonal and lamellar phases have also been observed.[4] These data show that block copolymers in general can form the same micellar structures as normal hydrocarbon surfactants do, that micelle formation is controlled by hydrophobic interaction, and that the phase diagrams are determined by packing constraints of hard-sphere objects.

The goal of the present investigation was therefore to study systematically the aggregation and phase behavior of the block copolymers in aqueous solutions as a function of the number of hydrophobic PO and hydrophilic EO units in the molecules. The results are compared with results on nonionic alkylpoly(glycol ether) surfactants.

2. Experimental Part

(a) Samples. The studied block copolymers are listed in Table 1 where their trade names, the numbers x and y, and their molar weights are given. The samples were gifts from BASF AG and Hoechst AG; they were used as received without further fractionation or other purification.

In order to check the composition and the molar weight distribution of the block copolymers, gel permeation chromatography experiments (GPC) were carried out on solutions of the samples in dimethylformamide (DMF) at 30 °C. In this solvent the block copolymers are dissolved as unimers and do not form micellar aggregates; this has been proven by dynamic light scattering measurements. In Figure 1 the obtained GPC curves are shown for PF 40 and F 127. Here the marked peaks are due to the block copolymer, while the other peaks come from the solvent.

A calculation of absolute molar weights from the GPC curves was not possible, because a standard $(EO)_x(PO)_y(EO)_x$ triblock copolymer with well-defined x- and y-values was not available. The GPC results show that the distribution of the molar weight of the samples is very broad and extends over 1 order of magnitude. The given molar weights in Table 1 represent therefore only average values. As can be concluded from the form of the peak for PF 40, this compound consists of triblock copolymers and does not seem to contain significant amounts of diblock copolymers or $(EO)_x$ or $(PO)_y$ polymers, while the shoulder of the peak for F 127 at the side of lower molar weights is very likely due to the presence of diblock copolymers.

Several procedures for the fractionation of the triblock copolymers have been described by Zhou and Chu[5] and by Booth et al.[6] In spite of the not well-defined composition of the samples, we decided to use the triblock copolymers as we had received

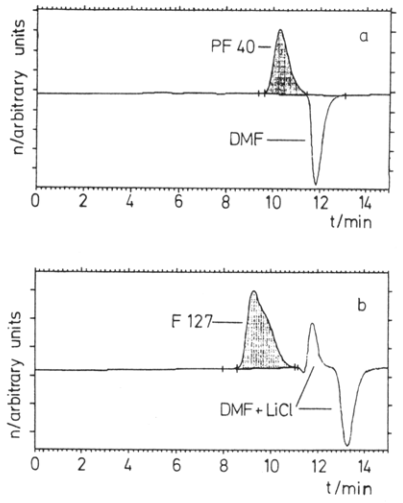

Figure 1. GPC curves of triblock copolymers in DMF solutions at 30 °C. The refractive index n as a function of the elution time t: (a) 5.23 g/L of PF 40; (b) 5.7 g/L of F 127.

them without making any attempt of fractionation. We had two reasons for this strategy. First, Booth et al.[6] had shown that the aggregation behavior of the fractionated compounds and the unfractionated samples did not differ significantly although some properties like the surface tension were strongly affected by the composition. Furthermore, we wanted to describe the behavior of the triblock copolymers as they can be received from the producer and as they are used for application. Otherwise, the results of various groups on the same sample could differ strongly and would depend on the applied purification process or could lead to confusing results. On the other hand, it can be expected that the available compounds show a rather constant composition; this can actually be seen in the present paper in Table 6 where the results of small-angle neutron scattering measurements show a satisfactory reproducibility for different samples of F 127.

(b) Methods. The gel permeation chromatography experiments were carried out with a Waters 150-C ALC/GPC apparatus which used a refractometer ERC-7512 for detection. The column contained a mixture of silica–Ti–fluoropolymer with a particle size of 5 μm and a pore size of 30 nm.

The surface and interfacial tension measurements were carried out using an automatic Lauda tensiometer KM 3 which was equipped with the ring method and a spinning drop tensiometer SITE from Krüss. The cmc values of the block copolymers in the aqueous solutions were determined from surface tension measurements.

Phase Diagrams. In order to establish the phase diagrams, many solutions were prepared from each compound in 5 wt % intervals. The compounds were weighted into calibrated test tubes of 1.5-cm diameter, and the water was then added to adjust for the concentration. The test tubes were then placed into a vibrator at low temperature until clear phases or a milky solution was obtained. The solutions were then put in a temperature bath and left to equilibrate for several days. When phase separation occurred, the two-phase system was homogenized and left for equilibration again. These steps were repeated several times until the same macroscopic phases were reproduced. The phases were checked for birefringence. The same procedure was then repeated for another temperature. In general, the temperature was changed in steps of 5 °C. For some systems intermediate concentrations were prepared and smaller temperature steps were used in order to determine the phase boundaries more accurately. For some samples with highly viscous and elastic properties, it was necessary to mix the systems at higher temperature and then keep the sample at the required temperature for equilibration.

The static light scattering measurements were carried out with a Chromatix KMX-6 laser photometer which allows determination of the intensities of the scattered light at scattering angles of 6° (forward scattering) and 174° (backward scattering). Light scattering experiments at intermediate scattering angles were performed with a Brookhaven light scattering apparatus which

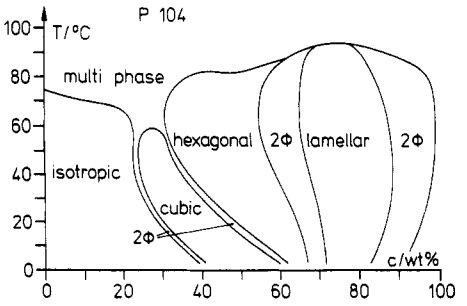

Figure 2. Phase diagram of the system P 104.

was also equipped with an autocorrelator for dynamic light scattering measurements. The refractive index increment dn/dc was determined with a Chromatix KMX-16 differential refractometer.

The SANS measurements were carried out in Grenoble at the Institute Laue-Langevin using the small-angle neutron scattering spectrometer D 11. This apparatus allows scattering measurements at a scattering vector between 0.001 and 0.3 Å^{-1}; the wavelength of the neutron beam can be varied between 5 and 10 Å with a half-width of 10%, and the distance between the sample and the detector can be chosen between 1 and 40 m. The x–y detector consists of 64 × 64 elements with a diameter of about 1 cm. The scattering intensity is monitored as a function of the scattering vector Q, and the curves are evaluated after calibration of the detector elements with an isotropic scatterer (H_2O) by comparison with the theoretical curves for different aggregates as is pointed out in section 3f.

The polarization microscopy measurements were made in order to identify the different lyotropic mesophases by their characteristic textures using a polarization microscope 18 Pol Standard from Zeiss in combination with a thermostating unit FP 80 and 82 from Mettler and a video system for automatic registration and documentation of the results.

The DSC measurements were carried out with a Perkin-Elmer DSC 7 apparatus and a Micro DSC apparatus from SETARAM which allows DSC measurements between 0 and 100 °C with an extremely high sensitivity and very low heating rates (to 0.1 °C/h). The micro-DSC allows measurements with sample masses up to 1 g and hence the detection of phase transitions with very small enthalpy values.

The ^{1}H-NMR measurements were carried on the block copolymer solutions in D_2O with a constant concentration as a function of the temperature using a Bruker AM 500 NMR spectrometer.

3. Results and Discussion

(a) Phase Diagrams. A phase diagram of P 104 is shown in Figure 2. This system forms all the different mesophases which are generally observed for normal hydrocarbon surfactants if the surfactant forms globular micelles in the L_1 phase. In the temperature range from 0 to 50 °C we observe first a cubic phase and then a hexagonal phase which is separated from the cubic phase by a two-phase region. For concentrations above 70 wt % a L_α phase is formed. Almost all liquid crystalline phases melt below 100 °C, and for even higher temperatures we find multiphase regions which separate into isotropic phases. The cubic, hexagonal, L_α phases could clearly be identified on their textures under the polarization microscope or by electron micrographs from TEM or by SANS measurements, respectively. We were not sure whether the region between the hexagonal and the L_α phases was a simple two-phase region or whether there was even another liquid crystalline phase as they are sometimes observed at this transition.[7]

In Figure 3 the phase diagrams of block copolymers are shown which all have the same PO block. We note that with decreasing size of the EO block the cubic phase and

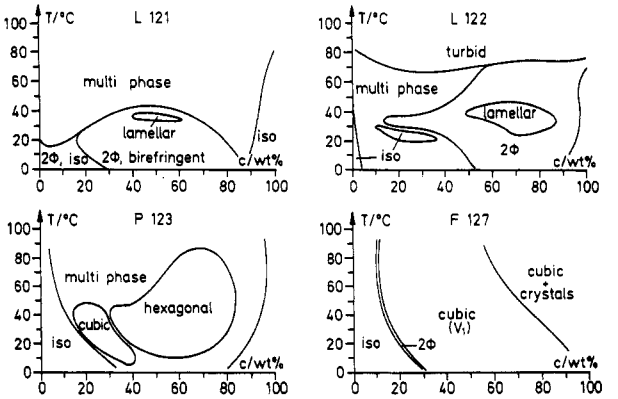

Figure 3. Phase diagrams of the systems of $(EO)_x(PO)_y(EO)_x$ block copolymers with y = 70 and x increasing from 5 to 106.

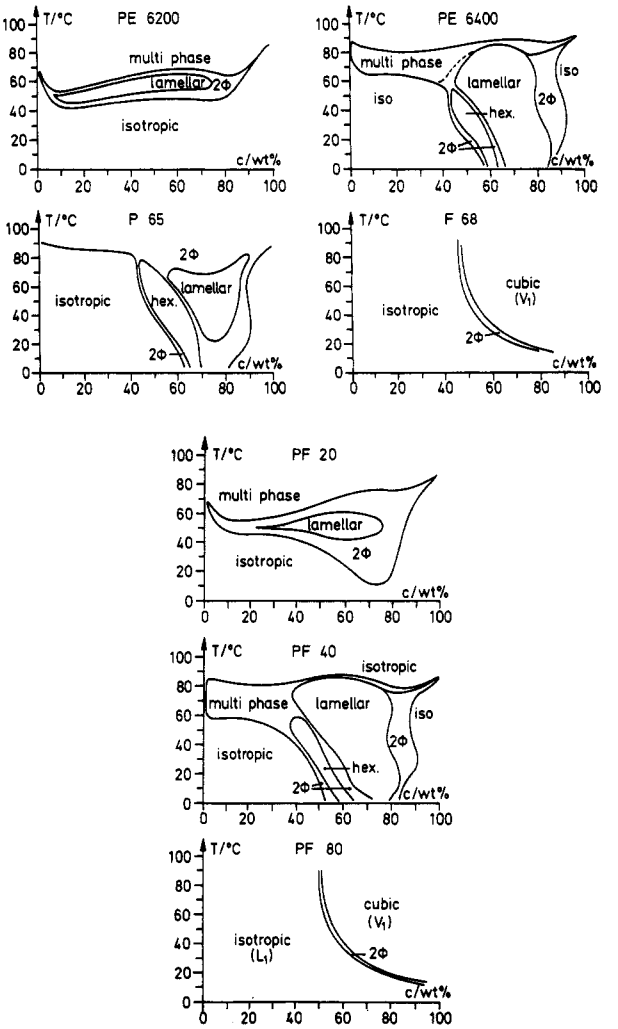

Figure 4. (a) Phase diagrams of the systems of $(EO)_x(PO)_y(EO)_x$ block copolymers with y = 30 and x increasing from 5 to 80. (b) Phase diagrams of the systems of $(EO)_x(PO)_y(EO)_x$ block copolymers with y = 27 and x increasing from 5 to 73.

then also the hexagonal phase disappear and finally the whole system is dominated by a L_α phase. This behavior is completely analogous to the phase diagrams of nonionic alkylpolyglycol ethers when the number of EO groups is reduced.[8]

Figure 4 shows phase diagrams where the PO block is again the same, but its size is somewhat smaller than in Figure 3. We again observe the same tendency. There is however one main difference with respect to the phase diagrams of simple nonionic surfactants. The phase boundaries of the normal surfactants are more or less

perpendicular in the T–C diagrams, while they run diagonal for the block copolymers. The mesophases of the block copolymers thus show a thermotropic behavior; the reversible transition of the isotropic solution to the mesophase or from one mesophase to the other can be brought about at constant concentration by increasing temperatures. This is obviously due to the fact that the compounds become much more lipophilic with increasing temperature; this will be discussed in more detail in section 3e.

The phase diagrams of Figure 4 furthermore show that the L_α phases for the block copolymers do not swell as much as those for the normal nonionics. Generally, it can be said that there are many similarities in the phase diagrams of normal surfactants and of block copolymers. It is likely that the block copolymers can form the same mesophases as do the normal surfactants. So far the nematic phase, the bicontinuous V_1 phase, and the L_3 phase have not yet been observed for the block copolymers. It is possible however that even these phases will be found if some of the systems are studied in more detail.

The macroscopic properties of the block copolymer mesophases are very similar to the properties of mesophases of normal surfactants. The cubic and hexagonal phases have a yield stress value which is high enough to prevent flow of macroscopic samples under the influence of the gravitational forces, while the lamellar phases in the studied systems either do not have a yield stress value or have only a much smaller yield stress value. This gives an additional possibility to distinguish the hexagonal from the lamellar phase. For example, the system P 104 forms a hexagonal phase at a concentration of 55 wt % and a lamellar phase at 70 wt % at room temperature. Contrary to the mesophases of other systems, these phases do not develop the typical textures under the polarization microscope but show only a weak and smooth birefringence. They also do not seem to flow in the gravitation field during an observation time of a few hours. But only the hexagonal phase does not flow over the time of several months, while the lamellar phase flows within 1–2 weeks. Larger air bubbles in the lamellar phase rise very slowly in several months, while smaller bubbles apparently do not move.

(b) Surface Tension Measurements. On first look at the results of surface tension measurements, the surface-active properties of the block copolymers seem to be similar to the ones of normal surfactants. For most systems one finds a concentration region in which the surface tension σ decreased linearly with the logarithm of the concentration until a critical concentration (cmc) is reached above which σ remains constant (Figure 5). From a single curve it would not be possible to differentiate a σ–log(c) curve for a block copolymer from the one for a normal nonionic surfactant.[9,10] Closer inspections of the details reveal however some important differences in particular for the temperature dependence. Surface tension measurements give three characteristic parameters: the absolute value of the surface tension at the cmc, the slope of the σ–log(c) curve before but close to the cmc, and the cmc. For hydrocarbon surfactants all three parameters are usually strongly correlated with each other. For the block copolymers the dependence of these quantities on molecular parameters seems to be different in some cases. This is particularly evident in the temperature dependence of the σ–log(c) curves. Such curves are given for P 104 in Figure 6. We find that the cmc changes strongly with temperature in a certain temperature range and so does the slope at the cmc. The absolute value of σ at the cmc changes however

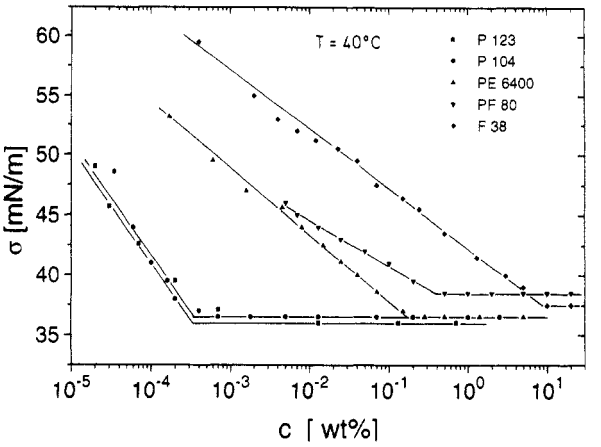

Figure 5. Surface tension σ for various block copolymer solutions as a function of the logarithm of the concentration at 40 °C.

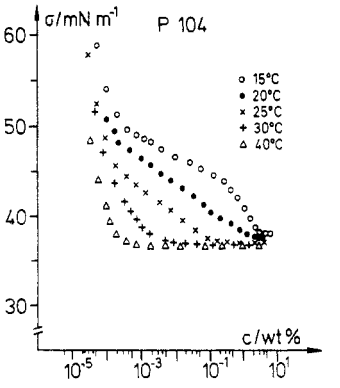

Figure 6. Surface tension σ for aqueous solutions of P 104 as a function of the concentration at various temperatures.

remarkably little for different temperatures. Using the Gibbs adsorption isotherm[11]

$$-\mathrm{d}\sigma = \Gamma_s RT\, \mathrm{d}\ln(c_s) \qquad (1)$$

where Γ_s is the surface concentration of surfactant molecules which are adsorbed at the surface and c_s is the bulk concentration of the surfactant, an area "A" per molecule can be calculated from the Γ_s values. These values are summarized in Table 2; they show that the area which a block copolymer occupies at the surface is decreasing with increasing temperature. It thus seems that the molecules become more compact. It is customary to calculate a heat of micellization from the temperature dependence of the cmc. These values are included in Table 4b in section 3e where they will be compared with the values which were obtained directly from the DSC measurements.

For a given temperature the cmc values depend on the length of the PO block. In Figure 7 a semilog plot of the cmc values is given against the number y of PO groups in the block copolymer. From this plot a linear relation between the logarithm of the cmc and y can be seen from which an energy $\epsilon \approx (0.2 - 0.3)kT$ for the transfer of a hydrophobic PO group from the aqeuous medium into the micellar interior can be calculated. This value agrees very well with the one which can be calculated from the cmc values of the block copolymers[2] according to the pseudophase model.[12] The cmc values for $C_y(EO)_6$ as a function of the number y of the CH_2 groups are included in Figure 7.[13] A corresponding energy for the transfer of a CH_2 group from the water into the micellar core can be derived from this linear plot which is $1.2kT$.[9,14] This value is 4–5 times higher than the value for a PO group. It can

Table 2. Values for the Surface Tension σ at the cmc, the cmc, the Surface Concentration Γ_s, and the Surface Area A at the cmc for Aqueous Solutions of Different Block Copolymers at Various Temperatures

system	T (°C)	σ (mN/m)	cmc (wt %)	Γ_s (mol/m²)	A (Å²/molecule)
F 38	40	37.5	7	8.8×10^{-7}	189
	25	39.7	10	7.97×10^{-7}	208
	20			7.44×10^{-7}	223
PF 80	45	38.4	4×10^{-1}	7.14×10^{-7}	233
	30	39.5	6	6.78×10^{-7}	245
	25	41.4	7	6.5×10^{-7}	256
	15			5.75×10^{-7}	289
PE 6200	40	36.4	2.3×10^{-2}	1.15×10^{-6}	145
	30	37.3	3	7.7×10^{-7}	216
	25	37.8		7.4×10^{-7}	225
	20			6.7×10^{-7}	248
	15			5.34×10^{-7}	311
PE 6400	40	36.3	1.5×10^{-1}	9.31×10^{-7}	178
	30	37.3	2.5	6.28×10^{-7}	264
	25	37.8	11	6.27×10^{-7}	265
	20			5.86×10^{-7}	283
	15			5.04×10^{-7}	330
P65	40	36.9	1.5×10^{-1}	8.8×10^{-7}	189
	30	37.0	3.2	6.67×10^{-7}	249
	25	37.8	8	6.0×10^{-7}	277
	15			5.3×10^{-7}	313
P 104	40	36.5	3×10^{-4}	2.66×10^{-6}	62
	30	36.9	2×10^{-3}	1.15×10^{-7}	145
	25	37.1	1.2×10^{-1}	5.32×10^{-7}	312
	20	37.8	1.5	4.74×10^{-7}	350
	15	38.2	2.5	3.86×10^{-7}	430
L 122	40	36.4	2.3×10^{-3}	1.59×10^{-6}	104
	30	36.4	4×10^{-3}	1.38×10^{-6}	120
	25	36.5	1.0×10^{-2}	1.07×10^{-6}	155
	15	37.6	7	3.8×10^{-7}	436
P 123	43	36.1	3×10^{-4}	4.57×10^{-6}	36
	35	36.3	1×10^{-3}	1.23×10^{-6}	135
	25	36.3	4×10^{-3}	8.26×10^{-7}	201
	17	36.5	4.5	4.63×10^{-7}	359
F 127	42	40.3	5×10^{-3}	1.39×10^{-6}	119
	15	40.6	7×10^{-1}	4.53×10^{-7}	366

thus be concluded that the hydrophobicity of a CH_2 group is 4–5 times stronger than that of a PO group. This is obviously due to the presence of the polar oxygen atom in the PO group.

Further information can be taken from Figure 7. An extrapolation of the line allows us to conclude that a block copolymer molecule must contain at least about 10 PO groups in order to be able to form micelles in aqueous solutions; compounds with smaller y-values will be dissolved as nonaggregating molecules. Due to uncertainties in the determination of the cmc values which come about from the broad distribution of both the x- and y-values of the block copolymers, the influence of the number x of the EO groups on the cmc cannot be determined. The cmc values of the nonionic surfactants $C_{10}(EO)_x$ increase slightly with increasing number x of EO groups;[13,15] Figure 7 shows, however, that in the case of the block copolymers the accuracy of the cmc values is not sufficient for such a statement.

From the DSC measurements in Table 4 (section 3e) it can be seen, however, that the temperature of micellization decreases with increasing size of the PO block and increases with increasing size of the EO block and that the latter effect becomes more pronounced for compounds with smaller PO blocks.

For temperatures below 15 °C several systems show a strange peculiarity of the σ–log(c) plots. At a concentration which is about an order of magnitude below the cmc the curves show a break which goes into the opposite direction as expected. The slope of the curves above this break is much steeper than that before the break and actually about

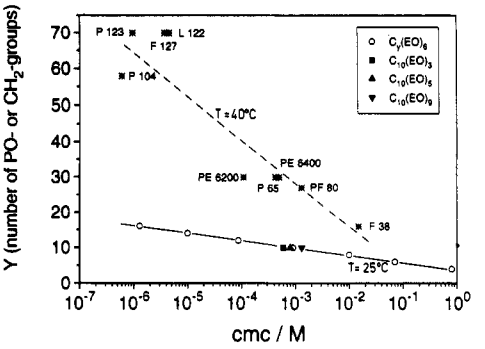

Figure 7. Logarithm of the cmc values for aqueous solutions of $(EO)_x(PO)_y(EO)_x$ block copolymers with different x-values at 40 °C and for aqueous solutions of alkylpoly(glycol ether) surfactants $C_y(EO)_6$ and $C_{10}(EO)_x$ at 25 °C as a function of the number y of the hydrophobic groups.

the same as the slope at the cmc for 40 °C. It is perhaps a coincidence; it is however observed for several systems. It seems that the molecules start to pack much more densely into the interface than below this concentration. It is not clear whether the break is the result of a change of the molecules in the bulk face or only in the interface. The break occurs at rather high concentrations at which the interaction between the molecules in the bulk must be considerable. It seems thus possible that the high osmotic pressure of the molecules leads to a collapse of the solvated molecules to a more dense state. It is thus conceivable that this break is due to a transition of solvated coils to micellar unimers in the bulk. At present there is no other information in support of such a transformation.

The absolute values of the surface tension at the cmc are rather high in comparison to normal hydrocarbon surfactants where values as low as 25 mN/m are known.[16] Furthermore, they do not depend very much on the number of EO groups having the same PO block as is shown for a series of compounds in Figure 5. The values increase somewhat with the number of EO groups but much less than for $C_y(EO)_x$ compounds.[10]

Summarizing the results of the surface tension measurements, it can be concluded that the hydrophobicity of the PO blocks increases strongly with increasing temperature which is indicated by the increasing surface activity and the decreasing cmc values. The strong decrease of the cmc with increasing temperature, which can be more than 4 orders of magnitude on a temperature increase from 15 to 40 °C, makes it useful to define a critical micellization temperature. In contrast, the cmc values of normal nonionic surfactants decrease only modestly with increasing temperature.[15]

This different behavior of the block copolymers is very likely due to a reversible dehydration of the PO units with increasing temperature; the hydrated PO groups show only weak hydrophobic properties, and their hydrophobicity increases significantly with the loss of water molecules. This conclusion is supported by Mortensen et al.,[17] who found a dissolution of block copolymer micelles into unimers with increasing pressure; this behavior is also shown by hydrocarbon surfactants.[18] It can be explained by a hydration of the hydrophobic groups which is favored by increasing pressure due to the smaller partial molar volume of the hydrated water in comparison to the free bulk water.[19] The decreased hydrophobicity of the hydrated hydrophobic groups can readily explain the increasing cmc. The reversible dehydration of the PO groups with increasing temperature is also in accordance with the very high positive enthalpy and entropy values

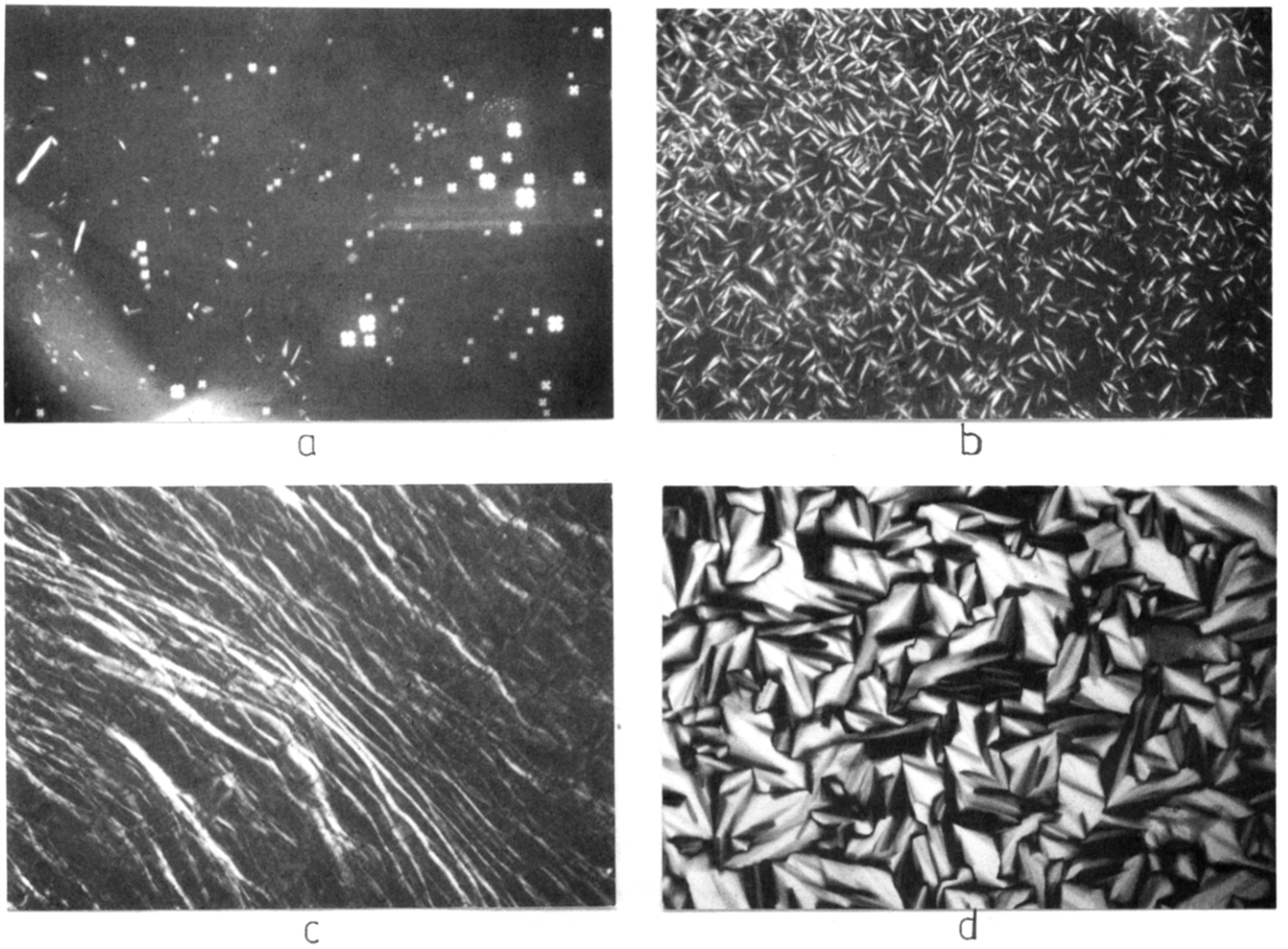

Figure 8. Textures under the polarization microscope of different lyotropic mesophases in binary systems of block copolymers and water: (a) spherolites of a lamellar phase in the two-phase region of 60 wt % PE 6200 at 54.2 °C; (b) batonets of a lamellar phase in the two-phase region of 60 wt % at 54.6 °C; (c) oily streaks of a lamellar phase of 70 wt % L 122 at 30 °C; (d) fanlike texture of a hexagonal phase of 57 wt % PE 6400 at 25 °C.

of the micelle formation as will be discussed further in section 3e.

(c) Polarization Microscopy. Lyotropic liquid crystalline phases are usually recognized on their texture under the polarization microscope.[20] This is also possible with the investigated systems even though the textures are not as distinct as for normal surfactants. One obvious reason for this probably has to do with the structure of the block copolymers. The interior of the micelles is probably much less ordered than that for single-chain hydrocarbon surfactants. For this reason the birefringence for the block copolymers is much weaker. Furthermore, the large-scale domain structure is less well-developed for the polymers than for the normal surfactants. Nevertheless, it is usually possible by tempering samples for a longer time under the polarization microscope to produce textures which show the characteristic features of the mesophases. Some of the pictures which were obtained are shown in Figure 8a–d. Figure 8a shows spherolites, and Figure 8b batonets of a forming lamellar phase in the two-phase region; Figure 8c presents oily streaks of a lamellar phase, and Figure 8d gives the fanlike texture of a hexagonal phase.

(d) Light Scattering Data. Detailed light scattering data have been reported by several groups on different $(EO)_x(PO)_y(EO)_x$ systems.[21] Most of these measurements had been carried out on rather dilute solutions of the polymer in order to avoid the micellar interaction. The main intention of this paragraph is to show that the change of the forward light scattering intensity and DSC measurements monitor the same process. Generally, one finds for all systems that for small concentrations the forward scattering intensity starts from a level which is due to the molecular weight of the block copolymer and increases with increasing temperature within a small temperature range and then levels off again to a more or less constant value. The temperature range where the main increase occurs depends somewhat on the system. This is also true for the small increase after the main transition. A typical plot for the forward scattering intensity is given in Figure 9a for a 5 wt % solution of P 104. The DSC signal for the same solution is shown in the same Figure 9a. This figure clearly shows that the light scattering intensity increases strongly in that temperature range in which the DSC peak occurs. This is of course no coincidence. Both methods monitor the same process. The height of the DSC signal gives us the amount of block copolymers which are transformed at a given temperature from the monomer to the micellar state. The light scattering for a given temperature and concentration monitors the mean molecular weight of the aggregates. In order to have a better comparison with the DSC curves, we should differentiate the R_θ values with T. Such a curve is given in Figure 9b. It has the same shape as the DSC curve. The peaks from the two curves are somewhat shifted with respect to each other, but otherwise they look alike. The shift could be due to the fact that the micellization process requires some time to reach equilibrium. Further DSC and light scattering data for different systems are summarized in

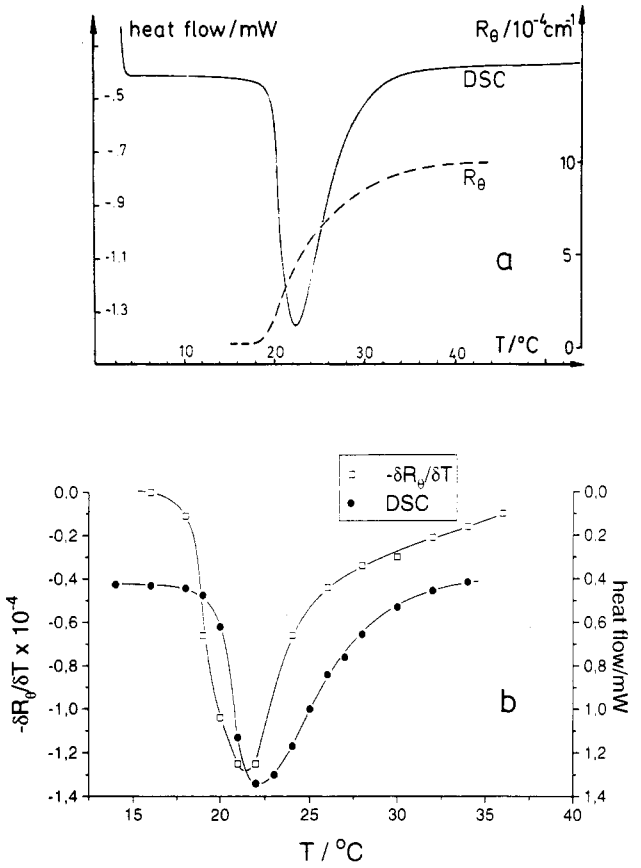

Figure 9. (a) Rayleigh ratio R_θ from static light scattering measurements (dashed line) and the heat flow from DSC measurements (drawn line) for a 5 wt % aqueous solution of P 104 as a function of the temperature. (b) First derivative $\delta R_\theta/\delta T$ of the Rayleigh ratio from the temperature and the heat flow for a 5 wt % aqueous solution of P 104 as a function of the temperature.

Figure 10. The data clearly show that the DSC signals are due to the micellization process. Some data which were evaluated from the light scattering data are summarized in Table 3.

For small concentrations of the block copolymers listed in Table 3 the molar weights and hence also the aggregation numbers n and dimensions of the aggregates are independent of concentration; these values decrease for concentrations above 10 wt %. This apparent decrease is due to the repulsive interaction between the micelles. The values in Table 3 show furthermore that below a characteristic temperature only monomeric block copolymer molecules which are also referred to as monomeric micelles exists in the solutions. At the characteristic temperature the aggregation of the unimers starts and the aggregation numbers of the micelles increase with increasing temperature within a range of 10–20 °C; with further increasing temperature the aggregation number of the micelles and hence the miceller size remains constant in a first approximation or increases slightly, respectively; similar observations have been made by Mortensen et al. (see refs[1] and [22]). This behavior is consistent with the results of the surface tension measurements which indicate that the PO blocks are little hydrophobic at low temperatures, and the block copolymers show a small surface activity and aggregation tendency. With increasing temperature dehydration of the PO blocks takes place, and the PO blocks become more and more hydrophobic which leads to micelle formation which is complete above a small temperature range.

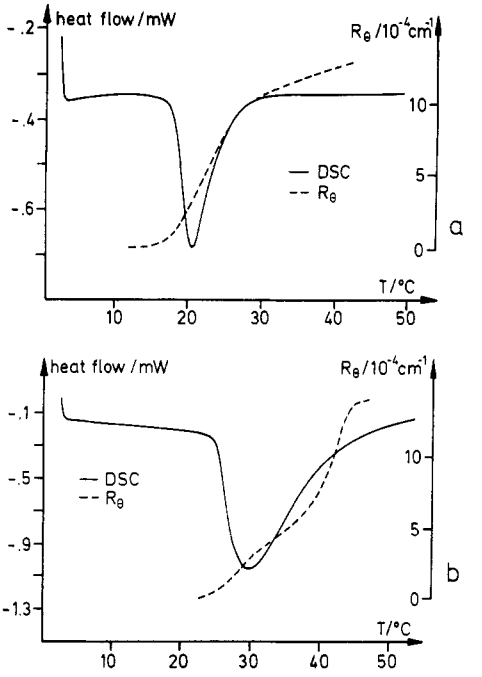

Figure 10. Rayleigh ratio R_θ from static light scattering measurements (dashed line) and the heat flow from DSC measurements (drawn line) for a 3 wt % aqueous solution of F 127 (a) and a 10 wt % aqueous solution of PE 6400 (b) as a function of the temperature.

Table 3. Values for the Molar Weights M_w, the Aggregation Numbers n, the Refractive Index Increments dn/dc, and the Radii R_{LS} of Spherical Aggregates in Aqueous Solutions of Various Block Copolymers at Different Temperatures Determined by Static Light Scattering Measurements with Extrapolation to Low Block Copolymer Concentrations

system	T (°C)	M_w	n	R_{LS} (Å)	dn/dc (mL/g)
PE6400	25	$\sim 3 \times 10^3$	~1		0.1393
	30	2.95×10^4	10	22.8	0.1355
	35	7.1×10^4	24	30.4	
	40	1.03×10^5	35	34.4	0.1271
	46	1.89×10^5	64	42.2	
P 65	25	$\sim 3 \times 10^3$	~1		0.1375
	32	1.3×10^4	4	17	
	36	3.8×10^4	11	24.5	0.1348 (35 °C)
	40	7.1×10^4	21	30.3	0.1278 (45 °C)
P 104	20	$\sim 8 \times 10^3$	~1		
	25	1.6×10^5	32	39	
	30	4.0×10^5	81	53.6	0.1283
	40	5.2×10^5	105	58.5	0.1254
	45	6.0×10^5	121	61.3	
P 123	20	$\sim 5 \times 10^3$	~1		
	25	5.0×10^5	86	57.7	0.1285
	27	1.23×10^6	211	77.9	
	35	1.42×10^6	244	81.8	
	40	1.67×10^6	287	86.3	
	45	1.73×10^6	297	87.3	
F 127	15	$\sim 1.5 \times 10^4$	~1		
	20	9.0×10^4	7	17	
	25	5.0×10^5	37	57	0.1341
	30	9.0×10^5	67	69.4	0.1282
	35	1.1×10^6	82	74	
	40	1.3×10^6	97	78.5	0.1259
	45	1.42×10^6	106	80.8	0.1240 (50 °C)

The hydrophilic parts of the systems PE 6400, P 65, and F 127 are not significantly smaller or in the case of F 127 even larger than the corresponding hydrophobic units; thus the formation of spherical aggregates in these solutions is in accordance with the theory of micelle formation.[23] For P 104 and especially for P 123 for which the hydrophobic part is almost twice as big as the hydrophilic part, a formation of anisometric micelles could

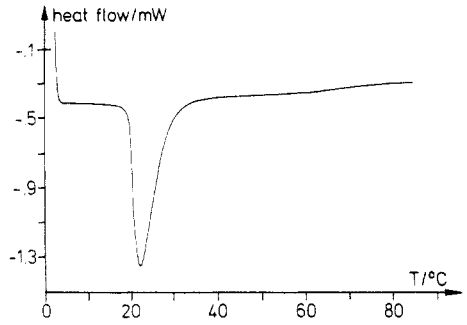

Figure 11. Transient DSC signal for the micelle formation in a 3 wt % aqueous solution of F 127.

be expected. The n values for P 123 solutions which are about a factor of 3 higher than the values for the other systems indeed suggest that anisometric micelles with an axial ratio slightly larger than 1 could be present in these systems. This assumption is supported by literature data on other related systems[1,22] but cannot be concluded unambiguously from the presented light scattering data and will be clarified by SANS measurements in the future.

A radius of the spherical micelles was calculated from the molar weights assuming that the density of the micelles is 1g/cm^3. The values are included in Table 3. These values show that the diameters of the micelles are smaller than the length of a fully stretched PO chain, if one takes 2.5 Å as the length of one PO unit and about 10 Å as the thickness of the hydrophilic shell of the micelles. This result is consistent with the existence of a spherical micelle in which the PO chains in the micellar core are not fully extended.[1,22]

In this context it should be mentioned that in electric birefringence measurements for the block copolymer solutions a signal could be detected which is larger than the signal of the pure solvent water. But this is not necessarily proof for the existence of anisometric particles, because the amplitude of the signal is usually very small in comparison to solutions with rodlike micelles and furthermore the time constant of the decay of the birefringence is a few hundred nanoseconds and hence equal to the time resolution of the apparatus. It is very likely, therefore, that the signal does not come about by the orientation of rodlike aggregates but by the orientation of segments of the polymer chains.

(e) DSC Measurements. (1) The Micellization Process. DSC measurements were carried out originally on block copolymer solutions the first time in order to obtain some information on the origin of the gelation process. No signal was observed, however, at the gelation temperature in the first measurements, but surprisingly a very large endothermic peak was found about 10 °C below the gelation temperature. A typical DSC signal of a F 127 solution is shown in Figure 11. It is characterized by the temperature at which the DSC curve has the maximum (T_m), the width of the peak at the base line (ΔT), and the integral heat (ΔH) below the signal. Detailed investigations later on showed that the endothermic peak could also be observed for solutions with concentrations below the sol–gel transition. These measurements showed furthermore that T_m decreased more or less linearly with increasing concentration. The origin of the DSC peak was not clear at its discovery. It was however assumed that it had something to do with the desolvation of the PO groups. In this investigation we made systematic DSC studies on all available samples; in particular we investigated how the DSC peak depended on the molecular weight of the PO and the EO block. We could observe DSC peaks for all studied systems. The typical parameters T_m, ΔT, and ΔH are summarized in Table 4a. The observed values for T_m vary from 8 °C for 25 wt % F 127 to 58 °C for 5 wt % PE 6800, and the ΔT values range from 14 °C for F 127 to 46 °C for P 65. We also observed again that for all samples T_m decreased linearly with the block copolymer concentration. The slopes vary for the different systems and are included in Table 4b as $\Delta T_m/\Delta c$; these values vary from −0.23 °C/wt % to −0.85 °C/wt % or from −47 °C/M to −800 °C/M, respectively. This table contains also the values for the heat ΔH of micellization for the different block copolymers which were calculated from the concentration dependence of T_m or from the temperature dependence of the cmc according to a van't Hoff plot.

The values in parts a and b of Table 4 show some systematic variations when we look at the details. Table 4a shows that the integral heat ΔH is in a first approximation directly proportional to the content of PO in the sample. This is clear evidence that the DSC peak is indeed a result of the desolvation of the PO groups. The average total heat of transformation per mole of PO is 3.0 ± 0.5 kJ/mol, and the ΔH values range from 0.8 kJ/mol of PO for PF 80 to 6.0 kJ/mol of PO for L 121. These values are rather high when we compare them with the ΔH values of other processes. The heat of melting of water, for instance, is 6 kJ/mol. It must be pointed out here that the exact determination of ΔT and hence also of the ΔH values is difficult due to the very broad DSC peaks. The Figures 9–11 show that the beginning and the end of the micelle formation process cannot be determined exactly. This is especially the case when T_m is lower than 15 °C because in this case the micelle formation starts already below 0 °C and hence outside of the measuring range of the DSC equipment.

From Table 4b it can be seen that the $\Delta T_m/\Delta c$ values increase in general with increasing x:y ratios. The table contains the ΔH values which were obtained from DSC measurements, from the slopes of the curves of $\ln(c_o) = f(1/T_m)$, where c_o is the total block copolymer concentration, and from the slopes of the curves of $\ln(\text{cmc}) = f(1/T)$. A comparison of these values shows in almost all cases a good agreement. It must be pointed out that the slopes of $\ln(\text{cmc} = f(1/T)$ show deviations from linearity especially for the sample with large PO blocks at higher temperatures. This behavior can be understood from the surface tension measurements which show that a dehydration process of the PO blocks takes place for these compounds in the temperature range below 30–35 °C which leads to an increased hydrophobicity of the PO block and hence to a promotion of the micelle formation. At higher temperatures the dehydration of the PO groups is practically complete and the temperature dependence of the cmc becomes smaller. Also the curves of $\ln(c_o = f(1/T_m)$ show deviations from linearity at higher concentrations above 20 wt %; this can be explained by the increased interparticle interaction in these highly concentrated systems which leads to similar ΔH values for the aggregation process. This can also be concluded directly from the DSC measurements which show that the ΔH values become generally smaller in the range of higher block copolymer concentrations.

The ΔH values in Table 4 decrease considerably for block copolymers with the same number of PO groups when the number of EO groups increases. The reason for this behavior might be that the EO groups can interact with the PO groups to a certain extent which increases with increasing x:y ratio; this interaction reduces the

Table 4. Values for the Temperature T_m at the Maximum of the DSC Peak, the Width ΔT of the DSC peak at the Base Line, and the Enthalpy ΔH of the Micellization Process for Various Block Copolymers at Different Block Copolymer Concentrations c_0 and Values for the Slopes $\Delta T_m/\Delta c$ and for the Enthalpies ΔH of the Micelle Formation Calculated from the Temperature Dependence of the cmc and from the Concentration Dependence of T_m for Various Block Copolymers $(EO)_x(PO)_y(EO)_x$

a. Values for T_m, ΔT, and ΔH

system	c_0 (wt %)	T_m (°C)	ΔT (°C)	ΔH (J/g)[a]	ΔH (kJ/mol)[b]
PF 20	20	23.3	28	9.6 ≡ 48	96.3 ≡ 75.2 (2.8)
	30	19.8	31	12.3 ≡ 40.9	82 ≡ 64 (2.4)
	40		36		
	52	15.9			
PF 40	5	31.4	30	2.9 ≡ 57.7	151 ≡ 84 (3.1)
	10	28.4	30	5.9 ≡ 58.8	154 ≡ 85.6 (3.2)
	20	24.1	36	9.8 ≡ 49.0	128 ≡ 71.4 (2.6)
	30	19.5	46	14.1 ≡ 47.0	123 ≡ 68.5 (2.5)
	40	11.1	42		
PF 80	10	40.6	38	1.33 ≡ 13.3	106 ≡ 20.7 (0.8)
	30	23.9	26	2.47 ≡ 8.24	66 ≡ 13
PE 6200	40	23.5	35	13.6 ≡ 34	74 ≡ 59 (2.0)
PE 6400	5	33.8	29	3.9 ≡ 78.2	232 ≡ 136 (4.5)
	10	29.9	34	5.3 ≡ 53.1	158 ≡ 92.4 (3.1)
	15	28.4	36	12.7 ≡ 84.7	252 ≡ 147 (4.9)
P 65	5	37.4	34	2.1 ≡ 42	147 ≡ 73.1 (2.4)
	10	34	34	2.9 = 29	102 ≡ 50.5 (1.7)
	20	30	38	7.0 ≡ 35	123 ≡ 61 (2.0)
	30	24.8	42	9.1 ≡ 30.2	106 ≡ 52.2 (1.8)
	40	20.4	46	9.8 ≡ 24.5	86 ≡ 42.6
	47	12			
PE 6800	5	57.7	37	0.7 ≡ 14	123 ≡ 24.5 (1.0)
	30	36.4	43	2.4 ≡ 8.0	71 ≡ 14
	40	27.7			
P 104	5	22.3	24	2.72 ≡ 54.4	269 ≡ 183 (3.2)
	10	20.1	29	5.34 ≡ 53.4	264 ≡ 180 (3.1)
	20	15.6	21	9.9 ≡ 49.6	245 ≡ 167 (2.9)
	30	10.0	25	12.7 ≡ 42.3	210 ≡ 143 (2.5)
L 121	1	17	24	0.93 ≡ 93.2	419 ≡ 377 (5.4)
	5	15.2	29.5	5.2 = 104	466 ≡ 421 (6.0)
	10	13.7	24	9.7 ≡ 96.5	434 ≡ 392 (5.6)
L 122	1	18.6	27	0.62 ≡ 62	310 ≡ 251 (3.6)
	10	15.3	23	8.0 = 80	402 ≡ 324 (4.6)
	15	13.9	23	11.3 ≡ 75.3	379 ≡ 306 (4.4)
	20	12.1	29	16.9 ≡ 84.4	424 ≡ 343 (4.9)
P 123	20	13.7	18	12 ≡ 60.3	351 ≡ 245 (3.5)
F 127	1	23.1	14	0.36 ≡ 36.2	485 ≡ 147 (2.1)
	2	21.9	15	0.74 ≡ 37.0	495 ≡ 150 (2.2)
	5	19.6	14	1.8 ≡ 36.1	483 ≡ 147 (2.1)
	10	16.9	15	3.5 ≡ 35.0	468 ≡ 142 (2.0)
	17	13.9	17	5.6 ≡ 33.0	441 ≡ 134 (1.9)
	18	12.8	17	5.7 ≡ 33.1	444 ≡ 135 (1.9)
	25	8.4	17	7.6 ≡ 30.5	409 ≡ 124 (1.8)

b. Values for $\Delta T_m/\Delta c$ and ΔH

system	y	x:y	$-\Delta T_m/\Delta c$ (°C/wt %)	$-\Delta T_m/\Delta c$ (°C/M)	ΔH^c (kJ/mol)	ΔH^d (kJ/mol)	ΔH^e (kJ/mol)
PF 20	27	0.19	0.23	47	96	90.4	
PF 40	27	0.44	0.47	122	154	151	
PF80	27	2.7	0.85	677	106	51.5	139
PE 6200	30	0.17			74		191
PE 6400	30	0.47	0.65	193	214	163	200
P 65	30	0.67	0.5	174	147	151	181
PE 6800	30	2.67	0.85	744	123	72	
P 104	58	0.31	0.84	416	269	231	346
L 121	70	0.07	0.38	171	397	520	
L 122	70	0.16	0.35	175	402	415	398
P 123	70	0.29			351		408
F 127	70	1.51	0.58	800	488	370	483

[a] The first value gives J/g of solution and the second J/g of block copolymer. [b] The first value gives kJ/mol for the block copolymer and the second kJ/mol for the PO block; the value in parentheses gives kJ/mol for one PO unit. [c] ΔH from DSC measurements at low concentrations. [d] ΔH calculated from the slope of the curves $\ln(c_0) = f(1/T_m)$. [e] ΔH calculated from the slope of the curves $\ln(\text{cmc}) = f(1/T)$.

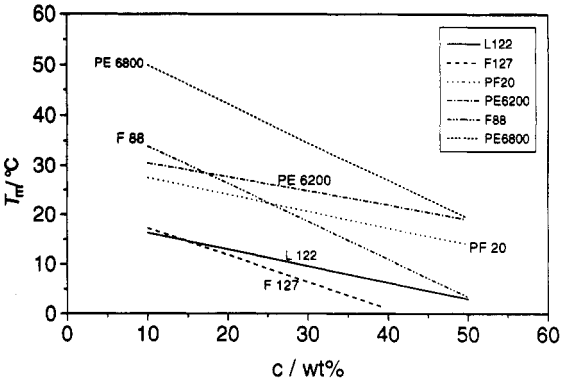

Figure 12. Temperature T_m at the maximum of the DSC peak for aqueous solutions of various block copolymers as a function of the block copolymer concentration.

hydration of the PO groups and hence also the energy of dehydration (see also below).

Since we associate the DSC peak with the PO groups, we should expect to find the same process in poly(oxypropylene) solutions without the EO groups. Indeed, we did observe a very broad peak for a 1 wt % solution of a poly(propylene oxide) with a molecular weight of 2000. The maximum of the peak was around 80 °C. No DSC peak was observed for solutions of poly(ethylene oxide).

The transformation temperature T_m depends on the molecular weight of the PO block and increases with decreasing molecular weight, as can be seen from Figure 12. The width ΔT of the peak is thus probably a reflection of the polydispersity of the PO block size. For monodisperse compounds we could expect a narrow peak and a broad peak for polydisperse particles. It is quite conceivable that a fractionation method for the systems could be developed which is based on the dependence of the micellization process on temperature. This fractionation process would require a method with which the micelles could be separated from the unimers which coexist with micellized block copolymer. Perhaps this could be possible by filtration through very fine micropore filters.

As already mentioned above and as shown in Figure 12 for some examples, the values of T_m for all block copolymers decrease linearly with increasing concentration. Figure 12 and Table 4b show furthermore that, in general, the absolute values of the slope $\Delta T_m/\Delta c$ are correlated with the x:y values; i.e., the curves for PE 6800 and F 88 (x:y ≈ 2.7) are practically parallel and have the highest slope, the curve for F 127 (x:y ≈ 1.5) has a considerably lower slope, and the curves for PF 20, PE 6200, and L 122 (x:y ≈ 0.16–0.18) are again almost parallel and have the lowest slopes. Plots of T_m as a function of the concentration of the hydrophilic PO units also show a linear decrease of T_m with increasing EO concentration but with high slopes for the samples with low x:y values and with low slopes for the EO-rich compounds. Finally, if T_m is plotted against the EO concentration and the PO concentration is taken into account with a factor of 0.1–0.15, all curves become parallel in a first approximation.

In the following an attempt is made to explain this behavior at least qualitatively. The decrease of T_m can be assumed to be due to hydration of both the EO and the PO units at sufficiently low temperatures. Thus with increasing block copolymer concentration, increasing amounts of water are bound which leads to a decrease of the chemical potential of free water and enhances the dehydration of the PO groups; consequently T_m must become lower with increasing concentration which is also consistent with the already mentioned slight decrease of ΔH_m with increasing block copolymer concentration.

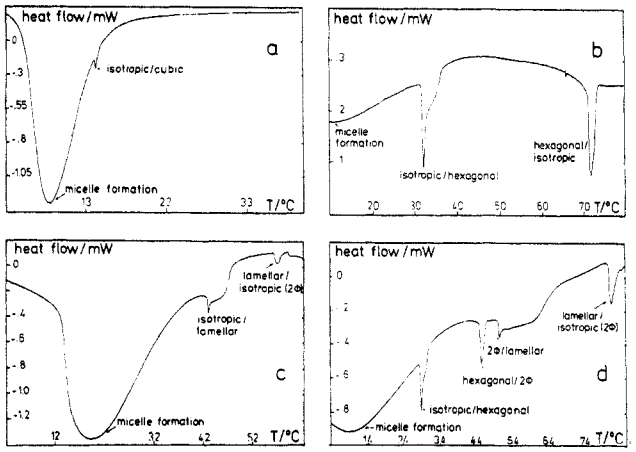

Figure 13. Transient DSC signals for various phase transitions in aqueous solutions of different block copolymers: (a) 25 wt % F 127, micelle formation and phase transition isotropic solution/cubic phase; (b) 50 wt % P 65, micelle formation and phase transition isotropic solution/hexagonal phase and hexagonal phase/isotropic solutions (multi-Φ); (c) 30 wt % PF 20, micelle formation and phase transition isotropic solution/lamellar phase and lamellar phase/isotropic solutions (multi-Φ); (d) 47 wt % PF 40, micelle formation and phase transition isotropic solution/hexagonal phase, hexagonal phase/two-phase region, two-phase region/lamellar phase, and lamellar phase/isotropic solutions (multi-Φ).

The stronger influence of the EO groups, i.e., the higher slopes of the $\Delta T_m/\Delta c$ curves of the EO-rich block copolymers, can be understood, because the EO groups are hydrated more effectively than the PO groups and their dehydration takes place at considerably higher temperatures in comparison to the PO groups.[24] Thus the PO blocks of samples with a high x:y ratio can be dehydrated more easily with increasing temperature than the PO units of compounds with a low x:y ratio which can explain the stronger decrease of T_m with increasing concentration for the EO-rich block copolymers. This explanation is supported by the result that the heat of dehydration per PO group decreases significantly from a value of about 6 kJ/mol for PO-rich block polymers to a value in the range of 1kJ/mol for EO-rich samples, as has been pointed out above already and can be seen from Table 4a.

It is necessary, however, in this context to mention a recent study of Lindman and Malmsten,[25] who found that increasing addition of poly(ethylene oxide) $(EO)_x$ to a cubic phase of F 127 leads to a "melting" of the gel. The $(EO)_x$ concentration which is necessary for the melting to occur decreases with increasing molar weight of the $(EO)_x$; addition of $(PO)_y$, on the other hand, stabilizes the cubic gel phase. This result leads to the conclusion that addition of $(EO)_x$ suppresses the micelle formation of the block copolymers and is thus contradictory to the generally observed decrease of T_m with increasing block copolymer concentration[1,5,26] and the explanation given above. The reasons for the influence of the block copolymer concentration on T_m are therefore not completely understood at present.

(2) Liquid Crystal Transitions. The phase diagrams in section 3a were determined by visual inspection of well-equilibrated samples with and without polarizers. Most of the mesophases which were identified in this way also give rise to a DSC peak. Typical DSC curves for several samples are shown in Figure 13a–c. From Figure 13b it can be seen that both the formation of the hexagonal phase of P 65 and the melting of this phase show up as an endothermic peak. Both processes are first-order phase transitions, and we can thus calculate a change of entropy for the process from ΔH according to $\Delta S = \Delta H/T$. The endothermic peak shows that the formation of the liquid crystalline phase from the isotropic micellar solution and the melting of the liquid crystalline phase are associated with an increase of the entropy. The situations are similar for the formation and melting of the cubic phase in Figure 13a and for the L_α phase in Figure 13c. A comparison of the results of the DSC measurements with the corresponding phase diagrams shows excellent agreement for all systems; this can be realized from the examples shown in Figure 13a–c. For example, the temperature at which the DSC peak indicates the transition of a 25 wt % solution of F 127 from the isotropic solution to the cubic phase agrees exactly with the temperature determined from rheological measurements at which the yield stress value and the storage modulus start to grow rapidly.[2]

No good theory seems to be available at present to explain the heat changes that are associated with the formation of lyotropic liquid crystals. Most theories actually treat the liquid crystalline formation of lyotropics on the basis of packing constraint in which only entropic contributions are assumed to the free energy.[27] Actually there is a lack of good experimental data on the thermodynamics of lyotropic liquid crystals in the literature. It is usually general practice to determine phase diagrams of thermotropic liquid crystals by DSC measurements and to determine from these experiments the enthalpy changes that are associated with the different phase transformations.[28] However, no systematic studies are known to us in which ΔH values have been determined for lyotropic liquid crystals. Usually it is assumed that these heat changes are very small. A few measurements have been made for the transition from the micellar solution to the nematics and from the nematics to the L_α phase;[29] the ΔH values for these phase transitions are very low and can be in the range of a few millijoules per gram solution.

Our results show that the ΔH values for the block copolymers are really not that small and 1–2 orders of magnitude higher than the corresponding values for phase transitions in liquid crystalline systems built up by normal hydrocarbon surfactants. However, they are still about 2 orders of magnitude smaller than the heat of micellization. The experimental data for the investigated systems are given in Table 5.

The heat of micellization is assumed to be mainly due to the desolvation of the PO groups. It is conceivable that the transitions of the different lyotropic mesophases contain contributions of this same basic process. With the exception of the cubic phase all other transitions are associated with a change of the number density of micelles and hence also with a change of the average curvature on the particles. The mesophase transitions require therefore some change in the solvation state of the block copolymers. For the formation and the melting of the cubic phase where such changes are absent we indeed observe smaller ΔH values than for the other phases. It is probably for this reason that the transition from the isotropic solution to the cubic phase was not detected in the first DSC measurements.

The ΔH values for the lamellar phases are much higher than those for the other mesophases. It is obvious from Figure 13c that the DSC peak for the formation of the lamellar phase is rather broad in comparison to the peaks for the other phase transitions which have only a width of a few degrees. The figure shows furthermore that the phase transition to the lamellar phase starts with a sharp peak within a small temperature range and extends then

Table 5. Values for the Temperature T_m at the Maximum of the DSC Peak, the Width ΔT at the Base Line, and the Heat ΔH of the Transformation of the Mesophases in the Binary System of $(EO)_x(PO)_y(EO)_x$ Block Copolymers and Water

system	c_0 (wt %)	T_m (°C)	ΔT (°C)	ΔH (J/g)[a]	ΔH (J/mol)[b]
		Phase Transition Isotropic Solution (or 2Φ) → Cubic Phase			
P 104	30	18	1	0.061 ≡ 0.203	1004 ≡ 683 (12)
	40	8.8	1.5	0.101 ≡ 0.252	1244 ≡ 846 (15)
P 123	35	13	1	0.053 ≡ 0.153	888 ≡ 515 (7)
F 127	25	14.3	1	0.025 ≡ 0.100	1335 ≡ 404 (6)
		Phase Transition Cubic Phase → 2Φ			
P 104	30	53.3	5	0.087 ≡ 0.29	1440 ≡ 976 (17)
P 123[c]	35	28.1	7.5	0.118 ≡ 0.337	1962 ≡ 1368 (19)
F 127	no phase transition from the cubic phase detectable up to 100 °C				
		Phase Transition Isotropic Solution (or 2Φ) → Hexagonal Phase			
PF 40	40	42	2	0.085 ≡ 0.21	558 ≡ 333 (12)
	45	30.5	3.5	0.202 ≡ 0.45	1180 ≡ 705 (26)
	47	28.9	3	0.18 ≡ 0.38	993 ≡ 595 (22)
	50	24.5	2	0.22 ≡ 0.43	1157 ≡ 673 (25)
	55	16.2	2	0.23 ≡ 0.42	1109 ≡ 662 (25)
	57	14.9	2	0.16 ≡ 0.28	722 ≡ 438 (16)
	70	no phase transition detectable between 0 and 100 °C			
	80	no phase transition detectable between 0 and 100 °C			
P 65	47	39.3	7	0.176 ≡ 0.37	1300 ≡ 644 (21)
	50	32.1	6.5	0.206 ≡ 0.41	1442 ≡ 713 (24)
	60	22.5	7.5	0.15 ≡ 0.25	875 ≡ 435 (15)
		Phase Transition Hexagonal Phase → Lamellar Phase through a 2Φ Region			
PF 40	40	56.3	13	0.63 ≡ 1.58	4149 ≡ 2474 (92)
	(40)[d]	(47.6)[d]	(3)[d]	(0.087 ≡ 0.22)[d]	(570 ≡ 345)[d]
	45	54	18	0.88 ≡ 1.96	5140 ≡ 3069 (114)
	(45)[d]	(48)[d]	(3)[d]	(0.175 ≡ 0.39)[d]	(1023 ≡ 610)[d]
	47	59.6	18	(0.79 ≡ 1.67)	4379 ≡ 2615 (97)
	(47)[d]	(45.6)[d]	(3)[d]	(0.141 ≡ 0.3)[d]	(784 ≡ 470)[d]
	(50)[d]	(44.5)[d]	(3)[d]	(0.16 ≡ 0.31)[d]	(818 ≡ 485)[d]
	55	38.3	9	*e*	*e*
	57	34.2	9	*e*	*e*
	60	30.5	9	*e*	*e*
P 65	60	67.9	5	0.145 ≡ 0.24	840 ≡ 418 (14)
		Phase Transition Hexagonal Phase → 2Φ (Isotropic)			
P 65	47	74.2	8	0.166 ≡ 0.35	1236 ≡ 614 (20)
	50	71.7	4	0.186 ≡ 0.37	1300 ≡ 644 (21)
		Phase Transition Isotropic Solution (or 2Φ) → Lamellar Phase			
PF 20	20	46	6	0.214 ≡ 1.07	2146 ≡ 1675 (62)
	30	43	7	0.44 ≡ 1.46	2935 ≡ 2292 (85)
	52	34.3	13	0.71 ≡ 1.37	2751 ≡ 2147 (80)
	63	21.3	15	0.61 ≡ 0.97	1942 ≡ 1516 (56)
	73	no phase transition detectable between 0 and 100 °C			
PE 6200	40	44.8	4.5	0.328 ≡ 0.82	1788 ≡ 1427 (48)
	70	40.2	4	*e*	*e*
		Phase Transition Lamellar Phase → One or More Φ			
PF 20	30	57.8	4	0.073 ≡ 0.24	488 ≡ 381 (14)
	52	58.8	4	0.22 ≡ 0.43	850 ≡ 673 (25)
	63	58.3	7	0.307 ≡ 0.49	978 ≡ 767 (28)
P 65	60	78.5	5	0.023 ≡ 0.038	134 ≡ 67
		Phase Transition Isotropic Solution → Isotropic Phase (Bicontinuous?)			
L 122	30	23.4	2	0.062 ≡ 0.21	1046 ≡ 853 (12)
		Phase Transition Isotropic Solution → Two or More Isotropic Phases			
PF 40	5	57.7	8	0.062 ≡ 1.24	3251 ≡ 2158
	10	56.9	10	0.193 ≡ 1.93	5060 ≡ 3358
	20	57.1	10	0.429 ≡ 2.15	5624 ≡ 3741
	30	56.8	11	0.61 ≡ 2.03	5323 ≡ 3532
PE 6400	5	60.7	8	0.071 ≡ 1.42	4226 ≡ 2471
	10	64.7	8	0.19 ≡ 1.9	5647 ≡ 3306
	15	60.4	11	0.28 ≡ 1.85	5508 ≡ 3219
		Phase Transition Two or More Isotropic Phases → Isotropic Solution			
PE 6400	10	85.1	5	0.053 ≡ 0.53	1575 ≡ 922

[a] The first value gives J/g of solution and the second J/g of block copolymer. [b] The first value gives J/mol for the block copolymer and the second kJ/mol for the PO block; the value in parentheses gives J/mol for one PO unit. [c] Phase transition to a hexagonal phase through a 2Φ region. [d] This peak is observed before the broad peak which is due to the formation of the lamellar phase; it might come from the transition from the hexagonal phase to the two-phase region hexagonal/lamellar. [e] Under these conditions was a peak so broad that ΔH values could not be calculated with sufficient accuracy.

more than 10 °C. The formation of the lamellar phase seems thus to be accompanied by a strong desolvation of the PO block which gives rise to the large ΔH values; the heat of melting of the lamellar phase which does not require such a desolvation is significantly smaller than the heat of formation.

(f) SANS Measurements. On a few selected block copolymer compounds SANS measurements were carried

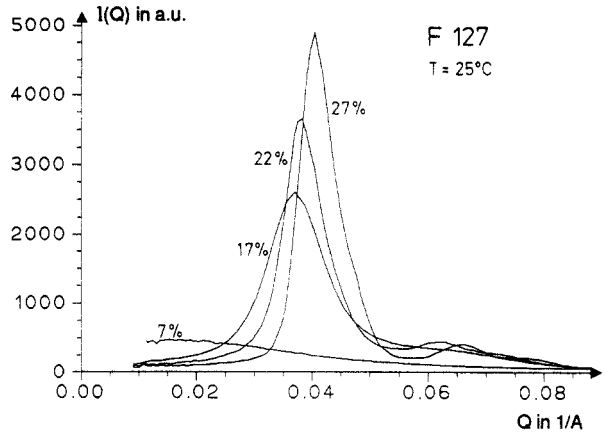

Figure 14. Radial average of the intensity $I(Q)$ of a scattered neutron beam from aqueous solutions with various concentrations of F 127 as a function of the scattering vector Q at 25 °C.

out in order to obtain information on the size, the shape, and the interaction of the micelles. Results of these measurements are given in Figure 14 for several concentrations of F 127 in linear intensity–scattering vector plots. The results show a strong correlation peak, the position of which is shifted to larger Q values with increasing concentration. This shows that the interaction between the micelles is repulsive. The aggregation numbers n and the radii R of the micelles were determined from the scattering data in three different ways, namely, from the form factor of isolated noninteracting spheres in the dilute range (R),[30] from the complete fit of the data assuming hard-sphere interaction (R_{HS}),[31] and finally from Q_{max} at the peak maximum at higher block copolymer concentrations (R_Q and n_Q);[32] in only one case also a fit for statistical coils was successful in the dilute range (R_G). The data are summarized in Table 6. For the system PE 6400 at 8 wt % which is below the cmc micelles were not observed. For concentrations high above the cmc we find that the aggregation number is practically independent of the block copolymer concentration up to the phase boundary of the hexagonal phase. Also for F 127 an independence of the aggregation number of the concentration and the temperature was found at high polymer concentrations, while for P 123 the aggregates increase with increasing temperature which was also found in the light scattering measurements. The results in Tables 3 and 6 show a good agreement for the data for the most studied systems; the only significant difference between the light scattering and the SANS data by a factor of 2 for the P 123 system can be understood easily if we assume that slightly anisometric particles are present in these solutions at 30 wt %. This can be seen also from the values for n which are found remarkably high also by the SANS measurements.

The independence of n of concentration for the other systems is best expressed in the linear plots of $(Q_{max})^3$ against the volume fraction Φ which is shown for F 127 in Figure 15. Such plots should be linear and have to go through the origin. This can easily be concluded from the following equations. Assuming that the correlation peak at Q_{max} is related to the nearest-neighbor spacing D between the particles by the approximation $D \approx 2\pi/Q_{max}$ and furthermore that each particle is surrounded by six nearest neighbors in a primitive cubic array, the number density N of the particles is approximately given by $N \approx (Q_{max}/2\pi)^3$. The number density can also be expressed by the volume fraction Φ, the molecular weight M_w of the particles, and their density ρ according to $N = N_L\rho\Phi/M_w$. We thus obtain $(Q_{max})^3 \approx N_L(2\pi)^3\Phi/M_w$.

As has been mentioned for the results of the light scattering data, the values for the diameters of spherical micelles derived from the SANS experiments are smaller than they are expected to be from the length of fully stretched PO chains. This indicates that the PO chains inside the micellar core are not completely extended.

Finally the structure factor $S(Q\rightarrow 0)$ was determined from the scattering data. The values are also given for P 104 in Figure 16 in a plot of $S(Q\rightarrow 0)$ against Φ_{eff}. The experimental points for all studied systems agree perfectly with the theoretical function for the structure factor if we assume that the effective volume fraction due to the hydration of the ether groups is a factorof 2–3 larger than the real volume fraction.

(g) ^{1}H-NMR Spectroscopic Measurements. NMR measurements were carried out on solutions of F 127 in D_2O as a function of the temperature in order to observe the possible changes of the signals which could be due to the aggregation of the block copolymer molecules and to the phase transition. Figure 17 shows the ^{1}H-NMR spectra of solutions of the block copolymer below the cmc and T_m, i.e., in the monomeric state, of pure poly(oxyethylene) $(EO)_x$ and of pure poly(oxypropylene) $(PO)_y$. It can be concluded from this figure that the sharp peak at ~3.5 ppm is due to the protons of the $(CH_2)_2$ units of EO, while the doublet at ~1 ppm belongs to the protons of the CH_3 groups and the broad peaks with the clearly visible hyperfine structure between 3 and 4 ppm come from the CH_2CH units of the PO; the sharp peak at ~4.5 ppm is the signal of HDO. The hyperfine structure of the broad peaks is caused by the coupling between the different protons of the CH_3 group, the CH_2 group, and the CH group and becomes still more complicated by the different possible configurations of the proton at the chiral CH group.

Figure 18 shows the ^{1}H-NMR spectra of a 1 wt % solution of F 127 in D_2O as a function of the temperature. It shows only the signals at ppm values beyond 3 ppm; i.e., it does not contain the signal for the CH_3 groups. From this figure the excellent agreement of the NMR measurements with the results of the other techniques can readily be seen. At low tempeatures the broad peaks of the CH_2CH units of the PO groups which are partially superimposed by the large peak of the $(CH_2)_2$ units of the EO groups show the described hyperfine structure; thus, it can be concluded that the block copolymer molecules are dissolved as unimers and hence the segments of the chains can move freely.

With increasing temperature the spectra do not change until the micellization temperature is reached. At this temperature the peaks which are due to the PO groups change drastically; the hyperfine structure disappears completely within a few degrees, the line width of the peaks increases and at least one of the peaks shifts towards lower ppm values. The peak which is due to the EO groups remains unchanged with increasing temperature. These features of the NMR spectra do not change with further increasing temperature. Similar results are obtained at higher concentrations of F 127 where the characteristic temperature is shifted toward lower values in agreement with the other results. These results show that the PO groups are transferred at T_m from the aqueous medium into the hydrophobic micellar core where due to the aggregation process they have a reduced mobility, while most the EO groups remain at the micellar surface and hence in contact with the solvent water.

Table 6. Values for the Radii R of Noninteracting Spherical Aggregates, the Radii R_{HS} of Spherical Aggregates with Hard-Sphere Interaction, the Radii of Gyration R_G of Statistical Coils, the Scattering Vectors Q_{max} at the Scattering Maximum, the Aggregation Numbers n, the Intermicellar Distances D, and the Radii R_Q of Spherical Aggregates Calculated from Q_{max} for Aqueous Solutions of Some Block Copolymers at Various Concentrations and Temperatures Determined from SANS Measurements

system	c (wt %)	T (°C)	R (Å)	R_{HS} (Å)	n	R_G (Å)	Q_{max} (Å^{-1})	D (Å)	n_Q	R_Q (Å)
PF 40	10	25	35.8		45					
	45	25					0.078 23	80.3	54	37.8
PE 6400	8	25	17.2		~4					
	20	25	26		15		0.049 73	126.3	82	45.4
	30	25					0.068 37	92.0	47	37.8
	40	25					0.076 9	81.7	44	37.0
	50	25		41.1	59		0.080 27	78.3	49	38.2
	55	25					0.084 81	74.1	hexagonal	
	60	25					0.084 26	74.6	hexagonal	
	70	25					0.091 11	69.0	hexagonal	
P 123	5	25	59.3		93					
	30	20					0.044 86	140.1	85	57.6
	30	30					0.042 56	147.6	100	60.7
	30	35					0.040 74	154.2	114	63.4
	30	40					0.040 13	156.6	119	64.4
	30	45					0.038 5	163.2	135	67.1
F127	1	25	49.6		24					
	3	25	46.3		18	35.5				
	5	25	48.5		22					
	7	25	49.3		23	49.5				
	12	25					0.031 07	202.2	45	61.2
	15	25					0.033 3	188.7	45	61.6
	17	25					0.033 28	188.8	51	64.3
	20	25					0.034 98	179.6	52	64.5
	22	25					0.035 75	175.8	54	65
	27	25					0.038 1	164.9	54	65
F127[a]	17	20					0.037 43	167.9	36	57
	17	25		65.4	54		0.037 43	167.9	36	57
	17	30					0.036 28	173.2	40	59
	17	45					0.036 27	173.2	40	59

[a] These measurements have been carried out with a different sample of F 127.

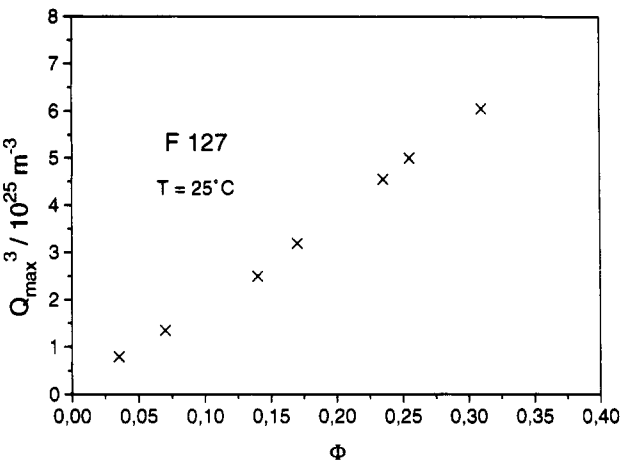

Figure 15. Third power of the scattering vector Q_{max} at the maximum of the intensity of a scattered neutron beam from aqueous solutions of F 127 as a function of the volume fraction Φ at 25 °C.

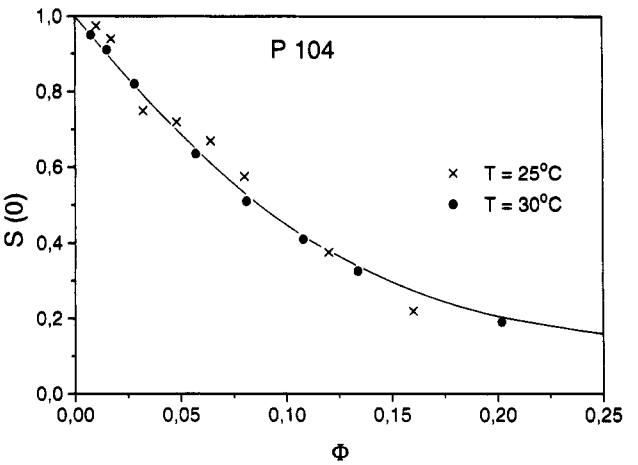

Figure 16. Structure factor $S(0)$ at a scattering vector $Q \to 0$ for aqueous solutions of P 104 as a function of the effective volume fraction Φ at various temperatures (the points represent experimental values; the drawn line the theoretically calculated values assuming hard-sphere interaction).

The agreement of the characteristic temperature for the NMR measurements with T_m of the other techniques shows furthermore that the replacement of H_2O by D_2O does practically not affect the aggregation behavior of the block copolymers. A similar conclusion can be drawn from the SANS measurements. The known phase behavior of the block copolymers in H_2O is not significantly changed by the switch to the solvent D_2O.

4. Conclusions and Comparison of the Results with Literature Data

At low temperatures the PO groups in the block copolymers have only weak hydrophobic properties as is indicated by the weak surface activity of the compounds. The block copolymers dissolve in water as unimers up to high surfactant concentrations. The low hydrophobicity is a result of hydration of the PO groups. With increasing temperatures the PO groups are dehydrated. The same conclusions were reached by Malmsten et al.,[33] who found increasing hydrophobicity of both poly(ethylene oxide) and poly(propylene oxide) with increasing temperatures in the ternary phase diagrams.

The increased hydrophobicity of the PO blocks which promotes the aggregation of the unimers to micelles is expressed in a dramatic decrease of the cmc by several orders of magnitude.[1,5,26] The hydrophobicity of the block copolymers is also dependent on pressure. Increasing

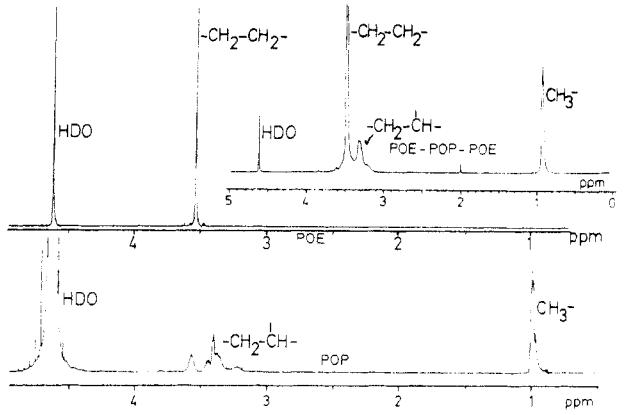

Figure 17. ^{1}H-NMR spectra of 1 wt % solutions of F 127, pure poly(oxyethylene), and pure poly(oxypropylene) in D_2O at 25 °C.

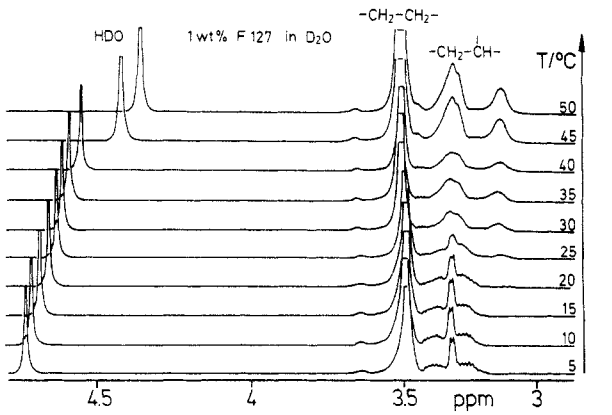

Figure 18. ^{1}H-NMR spectra of a 1 wt % solution of F 127 in D_2O at various temperatures.

pressure favors the hydration of the block conpolymers and consequently leads to a shift of the micelle–monomer equilibrium to the side of the monomers.[17,34]

Analoguous to normal surfactants, the cmc values for block copolymers are mainly determined by the length of the hydrophobic PO blocks. At least about 10 PO units are necessary for micelle formation.

The energy for the transfer of a PO group from the aqueous medium into the micellar core is in the range of about $(0.2–0.3)kT$.[2] This obviously means that the hydrophobicity of the C_3H_6 group in the PO group is almost completely compensated by the hydrophilic character of the polar–O–group.

Below the cmc and cmT unimers are present in the solution which are described as "monomeric micelles" in the literature.[1] Our results confirm the presence of unimers under these conditions but do not allow a conclusion to which extent they are coiled.

The structure of the micellar aggregates is similar to the structure of normal micelles; i.e., the hydrophobic PO groups are located in the micellar core which is surrounded by the hydrophilic shell formed by the EO groups; this model seems to be generally accepted by the different research groups[1,5,26] in spite of the results of Linse et al.[35] (see also ref 1), who conclude a modest miscibility of the PO and EO chains from experimental results.[33] Their model allows the presence of a few EO groups in the micellar core and also a few PO groups in the hydrophilic layer. They further assume that water molecules can penetrate into the hydrophobic core.

The aggregation of the block copolymers can be understood with the same model which was developed for normal surfactants.[23] Systems with relatively small hydrophobic groups and large hydrophilic groups form spherical micelles above the cmc; this was found for systems with $x:y \geq \sim 0.5$ by us as well as by other authors.[1,5,26] The radii of these micelles are practically independent of the concentration and also of the temperature if the temperatures are sufficiently high above cmT. The radii are somewhat smaller than the lengths of the completely stretched PO chains. These results are in accordance with studies of Mortensen et al. (see ref 1). These authors also found that for samples with significantly lower $x:y$ values anisometric micelles are formed with increasing temperature and concentration. It is likely from the presented phase diagrams that anisometric aggregates are indeed present in the isotropic micellar solutions which border on birefringent mesophases.

The micelle formation of the block copolymers is accompanied by a large positive heat which is proportional to the number of PO units in the molecules and is for one PO unit in the range of the heat of melting of water. Similar values have been found by Booth et al. (see ref 1). These large positive heat values which correspond to large positive entropy values for the micelle formation support further the conclusion that the micellization is accompanied by dehydration.

The sequence of the phases of the block copolymers is analogous to that of normal surfactants. For example, the phase sequence with increasing concentration is isotropic solution, cubic phase, hexagonal phase, and lamellar phase. Systems with $x:y \geq \sim 0.5$ form spherical micelles and a cubic phase as the first mesophase, systems with $x:y \approx 0.25$ form a hexagonal one, and systems with $x:y \approx 0.15$ form a lamellar one as the first mesophase. The macroscopic properties of these mesophases are similar to those of normal surfactants. The cubic and hexagonal phases have strong elastic properties and a yield stress value, while the lamellar phases either do not show a yield stress or have a much lower yield stress value.

There is also a significant difference to the phase behavior of normal surfactants. The phase diagrams show that the mesophases of the block copolymers show a marked thermotropic behavior. The different mesophases and the phase transitions can be produced at constant concentration with increasing temperature. The normal phase sequence on increasing temperature is again isotropic solution, cubic phase, hexagonal phase, and lamellar phase; for some systems the cubic phase and/or the hexagonal phase are absent, and a direct transition from the isotropic solution to the hexagonal or also to the lamellar phase can be found. These results are again in accordance with the literature data. For example, the formation of the cubic phase from an isotropic solution beyond a characteristic temperature is described as "inverse gel formation" or "inverse melting" by numerous authors and is attributed to come from hard-sphere interaction between the spherical micelles[36] (see also refs 1,5, and 26). The thermotropic transition from the cubic phase to the hexagonal one through a two-phase region is also described by Mortensen et al.[22,37] (see also refs 1 and 4) and by Linse;[35] in agreement with our results, the transition temperature decreases with increasing block copolymer concentration.

The thermotropic phase transitions have a positive heat of transition. The heat values are about 2 orders of magnitude smaller than the corresponding values for the micelle formation. Our results are consistent with corresponding literature data for the transition from the isotropic micellar phase to the cubic phase.[38] This transition is associated with an entropy increase in spite of the increase of the order of the aggregates. It is likely

that the phase transitions are accompanied by a small dehydration process of the PO units.

The lyotropic mesophases are stable only within a certain temperature range and "melt" again at temperatures below 100 °C, forming liquid systems which in most cases consist of more than two phases; similar observations have been made by Mortensen et al. (see refs 1 and 4).

Acknowledgment. Financial support of this work by the Deutsche Forschungsgemeinschaft, the Sonderforschungsbereich 213, the Fonds der Chemischen Industrie, and the European Community is greatfully acknowledged.

References and Notes

(1) Zhou, Z.; Chu, B. *J. Colloid Interface Sci.* **1988**, *126*, 171. Yu, G.; Deng, Y.; Dalton, S.; Wang, Q.; Attwood, D.; Price, C.; Booth, C. *J. Chem. Soc., Faraday Trans.* **1992**, *88*, 2537. Mortensen, K.; Pedersen, J. S. *Macromolecules* **1993**, *26*, 805. Brown, W.; Schillen, K.; Almgren, M.; Hvidt, S.; Bahadur, P. *J. Phys. Chem.* **1991**, *95*, 1850. Brown, W.; Schillen, K. *J. Phys. Chem.* **1992**, *96*, 6038. Linse, P.; Malmsten, M. *Macromolecules* **1992**, *25*, 5434. Malmsten, M.; Lindman, B. *Macromolecules* **1992**, *25*, 5446.

(2) Wanka, G.; Hoffmann, H.; Ulbricht, W. *Colloid Polym. Sci.* **1990**, *268*, 101.

(3) Almdal, K.; Bates, F. S.; Mortensen, K. *J. Chem. Phys.* **1992**, *96*, 9122. Mortensen, K. *Prog. Colloid Polym. Sci.* **1993**, *91*, 69.

(4) Yang, J.; Wegner, G.; Koningsveld, R. *Colloid Polym. Sci.* **1992**, *270*, 1080. Mortensen, K. *Europhys. Lett.* **1992**, *19*, 599.

(5) Zhou, Z.; Chu, B. *Macromolecules* **1988**, *21*, 2548.

(6) Wang, Q.; Yu, G.; Deng, Y.; Price, C.; Booth, C. *Eur. Polym. J.* **1993**, *29*, 665.

(7) Seddon, J. M. *Biochim. Biophys. Acta* **1990**, *1031*, 1. Tiddy, G. J. T. *Phys. Rep.* **1990**, *57*, 1.

(8) Mitchell, D. J.; Tiddy, G. J. T.; Waring, L.; Bostock, T.; McDonald, M. P. *J. Chem. Soc., Faraday Trans.* **1983**, *79*, 975.

(9) Shinoda, K.; Nakagawa, T.; Tamamushi, B.; Isemura, T. *Colloidal Surfactants*; Academic Press: New York, London, 1963.

(10) Cox, M. F. *J. Am. Oil Chem. Soc.* **1989**, *66*, 367.

(11) Gibbs, J. W. *Trans. Conn. Acad. Arts Sci.* **1876**, *3*, 375.

(12) Hartley, G. S. *Aqueous Solutions of Paraffin Chain Salts*; Hermann & Cie: Paris, 1936.

(13) Mukerjee, P.; Mysels, K. J. *Critical Micelle Concentrations of Aqueous Surfactant Systems*; NSRDS-NBS 26, 1971.

(14) Klevens, H. B. *J. Am. Oil Chem. Soc.* **1953**, *30*, 74.

(15) Corkill, J. M.; Goodman, J. F.; Harrold, S. P. *Trans. Faraday Soc.* **1964**, *60*, 202.

(16) Shinoda, K.; Yamanaka, T.; Kinoshita, K. *J. Phys. Chem.* **1959**, *63*, 648.

(17) Mortensen, K.; Schwahn, D.; Janssen, S. In *Annual Progress Report of the Department of Solid State Physics*; Pedersen, J. S., Lebech, B., Lindgard, P. A., Eds.; Risoe National Laboratory: Roskilde, Denmark, 1993; p 106. Mortensen, K.; Schwahn, D.; Janssen, S. *Phys. Rev. Lett.* **1993**, *71*, 1728.

(18) Tanford, C. *The Hydrophobic Effect*; John Wiley & Sons: New York, London, 1980. Desnoyers, J. E.; Roberts, D.; DeLisi, R.; Perron, G. In *Solution Behaviour of Surfactants*; Mittal, K. L., Fendler, J. E., Plenum Publishing Corp.: New York, 1982; Vol. 1, p 221.

(19) DeLisi, R.; Perron, G.; Desnoyers, J. E. *Can. J. Chem.* **1980**, *58*, 959. DeLisi, R.; Ostiguy, C.; Perron, G.; Desnoyers, J. E. *J. Colloid Interface Sci.* **1979**, *71*, 147.

(20) Hartshorne, N. H. *The Microscopy of Liquid Crystals*; Microscope Publications Ltd.: London, 1974. Demus, D.; Richter, L. *Textures of Liquid Crystals*; Verlag-Chemie: Weinheim, Germany, 1978. Mandell, L.; Fontell, K.; Lehtinen, H.; Ekwall, P. *Acta Polytechn. Scand.* **1968**, *74*.

(21) Almgren, M.; Bahadur, P.; Jansson, M.; Li, P.; Brown, W.; Bahadur, A. *J. Colloid Interface Sci.* **1992**, *151*, 157. Bahadur, P.; Nagar, T. N.; Rao, Y. K. *Tenside Surfactants Deterg.* **1992**, *29*, 121. Luo, Y. Z.; Nicholas, C. V.; Attwood, D.; Collett, J. H.; Prince, C.; Booth, C. *Colloid Polym. Sci.* **1992**, *270*, 1094.

(22) Mortensen, K.; Brown, W. *Macromolecules* **1993**, *26*, 4128.

(23) Israelachvili, J. N.; Mitchell, D. J.; Ninham, B. W. *J. Chem. Soc., Faraday Trans. 2* **1976**, *72*, 1525.

(24) Kjellander, R.; Florin, E. *J. Chem. Soc., Faraday Trans. 1* **77**, 2053.

(25) Malmsten, M.; Lindman, B. *Macromolecules* **1993**, *26*, 1282.

(26) Brown, W.; Schillen, K.; Hvidt, S. *J. Phys. Chem.* **1992**, *96*, 6038. Kausalya Reddy, N.; Fordham, P. J.; Attwood, D.; Booth, C. *J. Chem. Soc., Faraday Trans.* **1990**, *86*, 1569. Rassing, J.; Attwood, D. *Int. J. Pharm.* **1983**, *13*, 47. Rassing, J.; McKenna, W. P.; Bandyopadhyay, S.; Eyring, E. M. *J. Mol. Liq.* **1984**, *27*, 165.

(27) Danielsson, I. In *Lyotropic Liquid Crystals*; Friberg, S. E., Ed.; Advances in Chemistry Series 152; American Chemical Society: Washington, DC, 1976; p 13. Stenius, P.; Rosenholm, J. B.; Hakala, M. R. In *Colloid and Interface Science: Aerosols, Emulsions and Surfactants*; Academic Press: New York, 1976; Vol. 1, p 357. Rosenholm, J. B.; Hakala, M. R.; Stenius, P. *Mol. Cryst. Liq. Cryst.* **1978**, *45*, 285.

(28) Barrall E. M., II; Johnson, J. F. In *Liquid Crystals and Plastic Crystals*; Gray, G. W., Winsor, P. A., Eds.; John Wiley & Sons: New York, London, Sidney, Tokyo, 1974; Vol. 2, p 254.

(29) Hertel, G. Ph.D. Thesis, Universität Bayreuth, Bayreuth, Germany, 1989.

(30) Guinier, A. *Ann. Phys.* **1939**, *12*, 161. Guinier, A. *X-Ray Diffraction*; Freeman, H. W. & Cie: San Francisco, 1963. Porod, G. *Acta Phys. Aust.* **1948**, *2*, 255.

(31) Ashcroft, N. W.; Lekner, J. *Phys. Rev.* **1966**, *145*, 83.

(32) Hoffmann, H.; Thurn, H. In *Encylcopedia of Emulsion Technology*; Becher, P., Ed.; Dekker: New York, 1988; Vol. 3, p 171.

(33) Malmsten, M.; Linse, P.; Zhang, K. W. *Macromolecules* **1993**, *26*, 2905.

(34) Turro, N. J.; Kuo, P. L. *J. Phys. Chem.* **1986**, *90*, 4205. Camire, C.; Meilleur, L.; Quirion, F. *J. Phys. Chem.* **1992**, *96*, 2360.

(35) Linse, P. *J. Phys. Chem.* **1993**, *97*, 13896.

(36) Mortensen, K.; Brown, W.; Norden, B. *Phys. Rev. Lett.* **1992**, *68*, 2340.

(37) Mortensen, K. In *Annual Progress Report of the Department of Solid State Physics*; Pedersen, J. S., Lebech, B., Lindgard, P. A., Eds.; Risoe National Laboratory, Roskilde, Denmark, 1993; p 104.

(38) Deng, Y. L.; Yu, G. E.; Price, C.; Booth, C. *J. Chem. Soc., Faraday Trans.* **1992**, *88*, 1441. Luo, Y. Z.; Nicholas, C. V.; Attwood, D.; Collett, J. H.; Price, C.; Booth, C.; Chu, B.; Zhou, Z. K. *J. Chem. Soc., Faraday Trans.* **1993**, *89*, 539.